Determination of Photovoltaic Characteristics in Real Field Conditions

Seyedkazem Hosseini, *Student Member, IEEE*, Shamsodin Taheri, *Member, IEEE*, Masoud Farzaneh, *Life Fellow, IEEE*, Hamed Taheri, and Mehdi Narimani, *Senior Member, IEEE*

***Abstract*—This paper presents an improved procedure in the modeling of photovoltaic (PV) modules based on the single-diode model. This improvement allows more accurate energy yield predictions and performance analysis. Variation of parameters of the PV module model is taken into account, since the output characteristics depend on the surrounding conditions. The analytical expressions of the single-diode model along with experimental data are utilized to support the modeling approach. Moreover, the spectral effects, which influence the output of PV modules, are included in the model. Hence, the PV characteristics in real outdoor operating conditions could be precisely predicted. The effectiveness of the proposed procedure was tested against experimental measurements taken in a PV installation with different commercially available PV modules. The PV model was also validated using real data collected by the SCADA system of a 12-MW PV farm. A comparison with previous methods was made to show the advantages of the proposed model. This model can provide a powerful tool for analysis and appropriate selection of PV systems under changing environmental conditions.**

***Index Terms*—Photovoltaic (PV) modeling, photovoltaic systems, single-diode model, solar technologies.**

I. Introduction

IN RECENT years, photovoltaic (PV) energy has been one of the fastest-growing renewable energy generating technologies [1]. An effective electrical model of PV modules is needed for design and control of PV systems under various environmental conditions [2]. An electrical circuit is often employed to simulate the PV modules. This equivalent circuit is mainly based on single-diode [3], two-diode [4], or three-diode [5] models, as shown in Fig. 1. The effectiveness of the PV modeling in different ambient conditions depends on the accuracy of the circuit model parameters [6].

Many techniques were proposed in the literature to determine the parameters of the PV model. An iterative process is presented in [7] to obtain the PV model parameters. In [8], a generalized approach of PV array modeling based on the manufacturer datasheet is proposed. An equivalent PV circuit model is introduced in [9] to decrease the computational time. Moreover, soft computing methods based on evolutionary and swarm intelligence optimization techniques have been utilized to solve the problem [6], [10]. On the other hand, some studies present direct approaches to determine the parameters based on features of *P–V* and *I–V* curves. A symbolic procedure is developed in [11] to directly calculate the series and parallel resistors in the single-diode PV model using the Lambert W function. This function was also employed in [12] to provide an explicit PV string model, which can be used for energy yield calculations and partial shading conditions. Five parameters of the PV model are directly obtained in [13] by introducing a new coefficient.

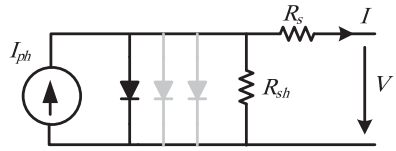

Fig. 1. Equivalent circuit model of the PV module.

Several studies have addressed variation of parameters of the PV model. A parameter extraction technique based on the single-diode circuit was investigated in [14]. However, the shunt resistance is adjusted to change solely with irradiance, and the series resistance is considered constant. In [15], the parameters of the PV model are extracted using manufacturer datasheets for several irradiance levels at 25 °C. The parameters are then arranged in a lookup table in order to update the parameters based on interpolation for different irradiance levels. However, the modeling technique is not applicable for outdoor operating situations where temperature and irradiance vary simultaneously. Moreover, explicit approaches have been proposed to determine the parameters of the single-diode PV model in different operating conditions. In [16], some main parameters of the PV model are translated at the first stage. Next, the variation of other unknown parameters is estimated. Explicit techniques are utilized in [17] to investigate the variation of parameters of PV panels in various operating conditions.

The existing PV modeling techniques consider a fixed solar spectral distribution where the air mass (AM) is set to 1.5 spectrum. However, in real field conditions, the AM and, consequently, the solar spectral distribution change over time.

Manuscript received November 11, 2017; revised December 24, 2017; accepted January 16, 2018. Date of publication February 9, 2018; date of current version February 16, 2018. *(Corresponding author: Seyedkazem Hosseini.)*

S. Hosseini and S. Taheri are with the Department of Computer Science and Engineering, Université du Québec en Outaouais, Gatineau, QC J8X 3X7, Canada (e-mail: hoss02@uqo.ca; shamsodin.taheri@uqo.ca).

M. Farzaneh is with the Université du Québec in Chicoutimi, Chicoutimi, QC G7H 2B1, Canada (e-mail: Masoud_Farzaneh@uqac.ca).

H. Taheri is with the École de Technologie Supérieure, Université du Québec, Montreal, QC H3C 1K3, Canada (e-mail: hamed.taheri64@gmail.com).

M. Narimani is with the Department of Electrical and Computer Engineering, McMaster University, Hamilton, ON L8S 4K1, Canada (e-mail: narimanm@mcmaster.ca).

Color versions of one or more of the figures in this paper are available online at http://ieeexplore.ieee.org.

Digital Object Identifier 10.1109/JPHOTOV.2018.2797974

2156-3381 © 2018 IEEE. Personal use is permitted, but republication/redistribution requires IEEE permission.
See http://www.ieee.org/publications_standards/publications/rights/index.html for more information.

Different PV technologies respond differently to this variation. As a result, different PV technologies would experience variation in their efficiency in real field conditions. However, this fact is not reported by manufacturers.

This paper builds on the initial study verified in [18]. The study is extended by providing both additional results of experimental measurements and further analysis and investigation of PV spectral and optical effects. This paper aims to develop an accurate model for predicting the electrical characteristics of the PV modules under real operating conditions. The uncertainties in environmental situations, which influence the values of the parameters of the circuit model, are examined. The proposed PV modeling technique, which is partially based on experimental data, updates the parameters to precisely predict the characteristics of the PV modules. Necessary corrections to the photocurrent are made through taking into account the AM and the angle of incidence (AOI) in the model. This can characterize the spectral and optical effects. The experimental results of outdoor measurements in conjunction with several comparative studies are used to verify the model. Furthermore, the capability of the proposed model in determining the annual energy yield of a 12-MW PV farm is assessed.

The rest of this paper is structured as follows. Section II discusses different PV technologies and the effect of changes in spectral distribution of sunlight. In Section III, different angles describing the position of the sun with respect to the surface of the PV panels are introduced. The detailed procedure of the proposed PV modeling technique is explained in Section IV. The validation of the proposed PV model is provided in Section V. This paper concludes with a discussion on the efficiency variation of different PV technologies.

II. Photovoltaic Technologies and Spectral Effect

Silicon, a type IV semiconductor, is the most popular material in PV technologies. Solar PV silicon would be either crystalline or amorphous. In the crystalline technology, the constituent silicon is a crystal with the thickness of around 0.1–0.2 mm. The amorphous technology is utilized as a thin film of around 1 μm thick deposited on a backing [19]. Other semiconductors, which are used in solar PV, are of types III–V such as gallium arsenide and thin films including cadmium telluride and copper indium selenide. Hence, there are two main groups of PV technologies: crystalline silicon (c-Si) materials that constitute 85–90% of the global market and thin films that represent 10–15% of global PV panel sales [20]. The c-Si cells are further divided into monocrystalline silicon and polycrystalline silicon (also called multicrystalline). This division actually depends on whether they are made up of a single crystal or of several assembled crystals.

The efficiency of the PV cells varies nonlinearly as the insolation level changes, which is not characterized by manufacturer datasheets. It has been shown in [21] that neglecting the variation of efficiency versus irradiance can cause errors in annual yield as high as 4.5%. PV panels respond only to a limited range of wavelengths. The spectral response of typical c-Si and amorphous silicon PV technologies is shown in Fig. 2 [19].

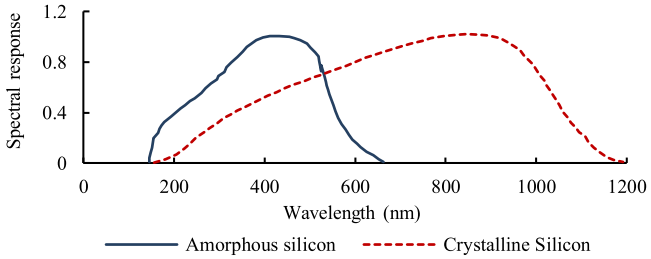

Fig. 2. Normalized spectral response of c-Si and amorphous silicon PV technologies.

The c-Si technologies have a better response in wavelengths of around 700–1100 (red and near-infrared portions), whereas the amorphous silicon responds well to short wavelengths of around 350–550 nm (blue and green portions). Furthermore, the spectral distribution of solar irradiance changes depending on the atmosphere and the position of the sun with respect to PV modules.

The AM, which continuously changes over time, has the major impact on the solar spectrum. For instance, the AM becomes higher as solar irradiance travels through more atmosphere. This will lead to a shift in solar spectrum toward longer wavelengths. As a result of different spectral responses, some PV technologies could benefit, but it might be disadvantageous for others. Nevertheless, the influence of variation of solar spectrum and PV devices spectral response has been largely neglected in PV module modeling.

III. Solar Angles

In order to realize the portion of sunlight converted to electricity, the position of the sun with respect to the PV module need to be assessed. This assessment would verify the angular relationship of solar rays, the earth, and the PV module at any time of a day and at any location. The solar angles formed between the sun and the earth are shown in Fig. 3. As can be seen from Fig. 3(a), the angle between a ray of the sun and the plane of the equator is defined as the "sun declination angle," δ, which can be estimated by a sinusoidal relationship [22]

$$\delta = 23.45 \ \sin\left[\frac{360}{365}(n-81)\right] \tag{1}$$

where n is the day number of a year starting from 1st of January ($n = 1$). This angle changes between the extremes of –23.45° (winter solstice, 21st of December) and +23.45° (summer solstice, 21st of June).

Fig. 3(b) illustrates the position of sun at any time of day in terms of two angles: the "sun altitude angle" β and the "sun azimuth angle" A. The sun altitude angle is defined as the angle formed between the sun ray and local horizon. The sun azimuth angle is normally measured in degrees off of due south and north for Northern Hemisphere and Southern Hemisphere, respectively. By convention, the sun azimuth angle takes positive values in morning when the sun is in the East and negative values in afternoon when the sun is in the West. The sun altitude

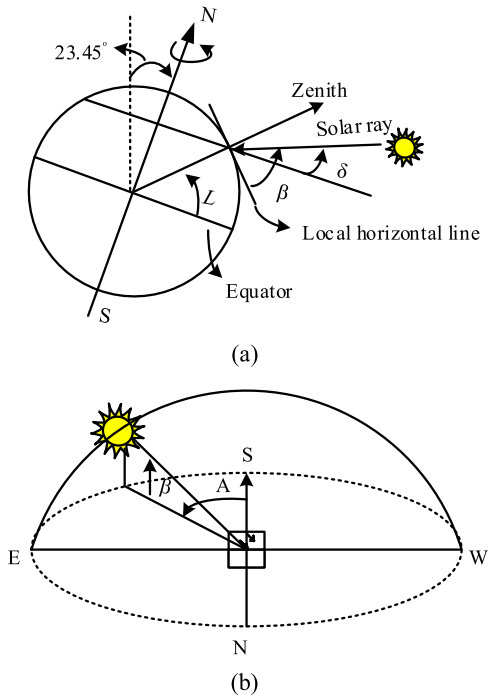

Fig. 3. Solar angles. (a) Altitude and declination angle of the sun. (b) Position of the sun in terms of azimuth and altitude angles.

and azimuth angle can be calculated as [23]

$$\beta = \sin^{-1}(\cos\ L\ \cos\delta\ \cos\omega + \sin\ L\ \sin\delta) \tag{2}$$

$$A' = \sin^{-1}\left(\frac{\cos\ \delta\ \ \sin\omega}{\cos\ \beta}\right)$$

$$\text{if}\ \ \cos\omega \geq \frac{\tan\delta}{\tan L}\ ,\ \text{then}\ \ A = \ A'$$

$$\text{otherwise},\ \ \cos\omega < \frac{\tan\delta}{\tan L}\ \ \text{and}\ A = \ 180 - A'. \tag{3}$$

Here, L is the latitude of a location on the earth, and ω, "hour angle," demonstrates the time of a day. The hour angle is the angular distance between the sun ray meridian and the local meridian. By taking into account that the earth rotates 15° per hour and a 24-h time scale for a day [22]

$$\omega = 15\,(12 - \text{ST}) \tag{4}$$

where ST is the solar time. In order to use (4), the local time should be converted to the solar time [24]. As can be observed from the aforementioned equations, the sun altitude and azimuth angles, i.e., the instantaneous position of the sun, depend on the latitude of a specific location, date, and time of a day. Another useful angle to be defined is the AOI, which is the angle between a normal to the PV module face and the direct sun ray and can be calculated as [22]

$$\text{AOI} = \cos^{-1}(\cos\ \beta\ \cos(A - \varphi)\sin\theta_T + \sin\ \beta\ \cos\theta_T) \tag{5}$$

where θ_T is the tilt angle of the PV module, and φ is the deviation of the PV module face from due South for Northern Hemisphere and due North for Southern Hemisphere. φ takes positive values toward the East and negative values toward the West. The AM is described as the mass of air through which the sun rays travel to reach a surface and is calculated as [24]

$$\text{AM} = \sqrt{(708\ \sin\ \beta)^2 + 1417} - 708\ \sin\beta. \tag{6}$$

Therefore, the AM changes depending on different days of a year, as well as different times of a day. This affects the intensity and spectral distribution of sunlight. Different PV technologies react differently to these variations.

IV. Proposed Methodology

The basic unit of a PV system is the PV cell that is composed of layers of semiconductors to convert the solar energy to electricity by directly absorbing the solar photons. Various PV cell technologies have various material arrangements and configuration designs, thus featuring different photo carrier transports. Nonetheless, PV cells can be electrically characterized by executing regular current–voltage tests. The equivalent circuit model of the solar module is shown in Fig. 1. An implicit equation characterizes the relationship between voltage and current of the single-diode PV model as

$$I = I_{\text{ph}} - I_s\left[\exp\left(\frac{V + R_s I}{a V_t}\right) - 1\right] - \frac{V + R_s I}{R_{\text{sh}}}. \tag{7}$$

In this equation, R_s is the series resistor, R_{sh} is the shunt resistor, a is the ideality factor of the model diode, I_{ph} is the photogenerated current of the PV module, I_s is the diode saturation current, and $V_t = N_s k T_c/q$ is the thermal voltage of the solar module, as T_c is the p-n junction temperature in Kelvin, $q = 1.60217646 \times 10^{-23}$ C is the charge of an electron, $k = 1.3806503 \times 10^{-23}$ J/K is the Boltzmann constant, and N_s is the number of solar cells connected in series. To thoroughly describe a solar module, the model requires a set of five parameters, i.e., R_s, R_{sh}, I_{ph}, I_s, and a. A systematic approach is proposed here to derive the parameters so that the model can be updated for arbitrary atmospheric conditions.

A. Updating I_{ph} and I_s

As insolation generates the photocurrent of PV cells, and its measurement is the primary source of error when evaluating the solar modules characteristics. Soiling, for example, can result in a steady decrease in the measured current of the solar modules. The photocurrent is basically impacted by the solar irradiance density hitting the surface of the PV module and marginally influenced by temperature. The photocurrent of the PV module I_{ph} can be precisely calculated as [21]

$$I_{\text{ph}} = f\,(\text{AM})\,.\,f\,(\text{AOI})\,.\frac{G}{G_{\text{STC}}}.K_{sf}\ \left[I_{\text{ph,STC}} + K_I\,(T_c - T_{\text{STC}})\right] \tag{8}$$

where G is the solar irradiance, and $f(\text{AM})$ and $f(\text{AOI})$ characterize the impact of changes of the solar spectral distribution and optical losses, respectively. K_{sf} quantifies derating of PV cells because of factors such as aging and dirt. T_c is the p-n junction temperature, K_I is the temperature coefficient of the short-circuit current provided by manufacturers, and $I_{\text{ph,STC}}$ is

the photocurrent of the PV module at STC, in which the irradiance level is $G_{\mathrm{STC}} = 1000\ \mathrm{W/m^2}$, the temperature of PV cells junction is $T_{\mathrm{STC}} = 25\ ^{\circ}\mathrm{C}$, and the solar spectral distribution is set to an AM = 1.5 spectrum. $I_{\mathrm{ph,STC}}$ will be calculated by writing (7) for short-circuit condition. $f(\mathrm{AM})$ and $f(\mathrm{AOI})$ can be obtained as [25]

$$f(\mathrm{AM}) = a_0 + a_1(\mathrm{AM}) + a_2(\mathrm{AM})^2 + a_3(\mathrm{AM})^3 + a_4(\mathrm{AM})^4 \tag{9}$$

$$f(\mathrm{AOI}) = b_0 + b_1(\mathrm{AOI}) + b_2(\mathrm{AOI})^2 + b_3(\mathrm{AOI})^3 + b_4(\mathrm{AOI})^4 + b_5(\mathrm{AOI})^5. \tag{10}$$

The coefficients of (9) and (10), i.e., a_0–a_4 and b_0–b_5, for different solar modules can be achieved from the module database available in [26], or by regression methods using real operating measurements. Therefore, to obtain the photogenerated current, (8) realizes the effective irradiance, i.e., the irradiance that is converted to electricity. The following relationships are obtained by applying the short-circuit and the open-circuit conditions to (7) at STC:

$$I_{\mathrm{ph,STC}} = I_{\mathrm{sc,STC}} + I_{s,\mathrm{STC}}\left[\exp\left(\frac{R_s I_{\mathrm{sc,STC}}}{aV_t}\right) - 1\right] + \frac{R_s I_{\mathrm{sc,STC}}}{R_{\mathrm{sh}}} \tag{11}$$

$$I_{\mathrm{ph,STC}} - I_{s,\mathrm{STC}}\left[\exp\left(\frac{V_{\mathrm{oc,STC}}}{aV_t}\right) - 1\right] - \frac{V_{\mathrm{oc,STC}}}{R_{\mathrm{sh}}} = 0 \tag{12}$$

where $I_{\mathrm{sc,STC}}$, $I_{s,\mathrm{STC}}$, and $V_{\mathrm{oc,STC}}$ are the short-circuit current, the reverse saturation current of the diode, and the open-circuit voltage under STC, respectively. The short-circuit current $I_{\mathrm{sc,STC}}$ and open-circuit voltage $V_{\mathrm{oc,STC}}$ are provided by manufacturer datasheets. By substituting (11) into (12), the reverse saturation current of the diode $I_{s,\mathrm{STC}}$ can be calculated as

$$I_{s,\mathrm{STC}} = \frac{\left\{\frac{(V_{\mathrm{oc,STC}} - R_s I_{\mathrm{sc,STC}})}{R_{\mathrm{sh}}} - I_{\mathrm{sc,STC}}\right\}}{\left\{\exp\left(\frac{R_s I_{\mathrm{sc,STC}}}{aV_t}\right) - \exp\left(\frac{V_{\mathrm{oc,STC}}}{aV_t}\right)\right\}}. \tag{13}$$

Consequently, the photogenerated current of the PV module I_{ph} can be updated by (8). The PV module output voltage is mainly influenced by temperature and slightly by the level of irradiance. However, the effect of irradiance becomes more significant at low irradiance levels. As a result, the open-circuit voltage is calculated as a function of both cell temperature and insolation as [27]

$$V_{\mathrm{oc}} = V_{\mathrm{oc,STC}} + aV_t \ln(G_{\mathrm{eff}}) + K_V(T_c - T_{\mathrm{STC}}) \tag{14}$$

where K_V is the temperature coefficient of the open-circuit voltage available from manufacturer datasheet, and G_{eff} is the effective irradiance ratio introduced as

$$G_{\mathrm{eff}} = f(\mathrm{AM}).f(\mathrm{AOI}).G.K_{sf}/G_{\mathrm{STC}}. \tag{15}$$

Therefore, the diode reverse saturation current I_s is dependent on both temperature and irradiance and is updated as

$$I_s = \left(I_{\mathrm{ph}} - \left(V_{\mathrm{oc,STC}} + aV_t \ln(G_{\mathrm{eff}}) + K_V(T_c - T_{\mathrm{STC}})\right)/R_{\mathrm{sh}}\right) / \left(\exp(V_{\mathrm{oc}}/aV_t) - 1\right). \tag{16}$$

B. Updating R_s and R_{sh}

The maximum power point (MPP) of the *I–V* curve varies nonlinearly as the temperature and the irradiance level change. The voltage and current of the MPP of a PV module in different atmospheric conditions can be estimated as [25]

$$I_m = \left(C_0 G_{\mathrm{eff}} + C_1 {G_{\mathrm{eff}}}^2\right).\left(I_{m,\mathrm{STC}} + K_{Im}(T_c - T_{\mathrm{STC}})\right) \tag{17}$$

$$V_m = V_{m,\mathrm{STC}} + C_2 aV_t \ln(G_{\mathrm{eff}}) + \frac{C_3(aV_t \ln(G_{\mathrm{eff}}))^2}{N_s} + K_{Vm}(T_c - T_{\mathrm{STC}}) \tag{18}$$

where $V_{m,\mathrm{STC}}$ and $I_{m,\mathrm{STC}}$ are the voltage and current of the MPP at STC, respectively, provided by the manufacturer datasheet. K_{Vm} and K_{Im} are the MPP voltage and current temperature coefficients, respectively. K_{Vm} and K_{Im} together with other coefficients of (17) and (18), i.e., C_0–C_3, can be achieved for different solar modules from the module database, or by regression methods from real operating measurements. Using (17) and (18), the MPP of the PV characteristic can be updated as $P_{m,\mathrm{cal}} = V_m \times I_m$ for arbitrary ambient conditions. The series and parallel resistances of the model, R_s and R_{sh}, are obtained such that the estimated MPP $P_{m,\mathrm{cal}}$ is equal to the MPP of the modeled PV characteristic. The following equation for R_{sh} is derived from (7) by applying the MPP condition

$$R_{\mathrm{sh}} = \frac{V_m(V_m + R_s I_m)}{V_m I_{\mathrm{ph}} - V_m I_s \exp\left(\frac{V_m + R_s I_m}{aV_t}\right) + V_m I_s - P_{m,\mathrm{cal}}}. \tag{19}$$

By initializing the two parameters as

$${R_s}' = 0, \quad {R_{\mathrm{sh}}}' = [V_m/(I_{\mathrm{sc}} - I_m)] - [(V_{\mathrm{oc}} - V_m)/I_m] \tag{20}$$

the standard Newton–Raphson iterative method is used to calculate the resistors. In each iteration of the iterative procedure, R_s is increased slightly with a predefined step-size and R_{sh} is calculated simultaneously by (19) up until the criterion at the MPP is satisfied. Therefore, the two resistances of the model R_s and R_{sh} are updated for arbitrary atmospheric conditions.

C. Determining Diode Ideality Factor

The diode ideality factor a indicates the extent of ideality of the circuit model diode and its value resides in a known range (e.g., $1 < a < 2$ for monocrystalline and polycrystalline silicon). By adopting an arbitrary value of a and calculating the other four parameters, the *I–V* and *P–V* curves would cross through the three major points provided by the manufacturer datasheet. Nonetheless, a proper value of a is required to appropriately model the remaining of the PV characteristics. In this paper, the diode ideality factor is obtained based on the fitting approach proposed in [15]. Scanning different values of a within its allowable range while determining four other parameters produces different sets of five parameters. The best set among these sets is the one with the minimum difference between the measured *I–V* curve (possibly at STC) and the modeled one. The diode ideality factor associated with the best set is then derived.

To realize the development of PV characteristics, a simplified algorithm in Fig. 4 illustrates the proposed technique in

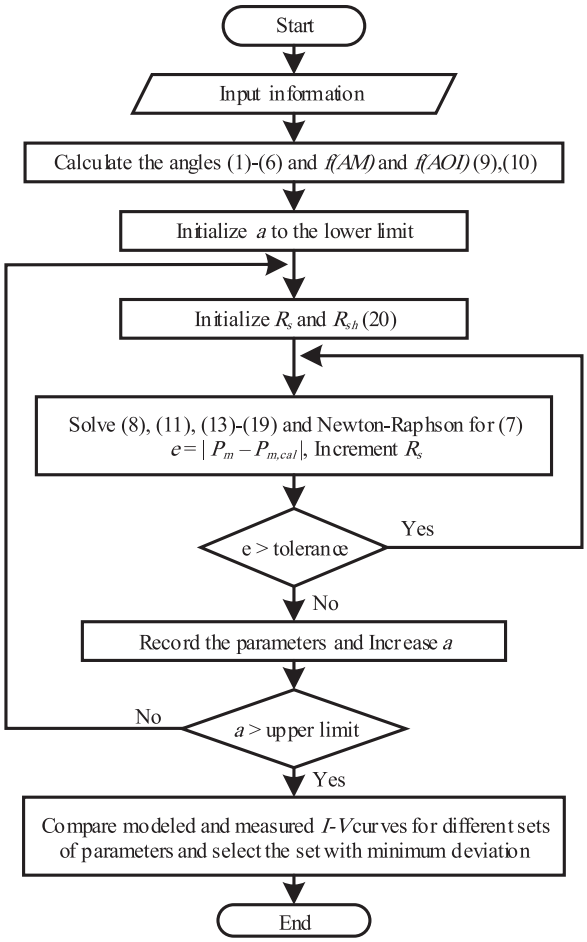

Fig. 4. Algorithm of the proposed technique.

conjunction with the criterion of the iterative approach. The input data contain temperature, irradiance level, module database, manufacturer datasheet, and field information. In the iterative process, the condition to reach the estimated MPP is checked, and if it is satisfied, the parameters of the model are derived. Otherwise, the procedure proceeds by an increment in R_s, and new parameters will be obtained.

V. Results and Model Validation

This section studies the effectiveness of the proposed approach in characterizing the real performance of PV modules under varying ambient conditions.

A. Parameter Variation

The impact of temperature and insolation levels on the parameters of the PV module model is investigated in this section. The short-circuit current is primarily dependent on irradiance and increases (decreases) as irradiance level increases (decreases). On the other hand, temperature primarily influences the output voltage of the PV module. As the temperature decreases, the open-circuit voltage increases, while the output current decreases slightly and vice versa. The open-circuit voltage is slightly affected by variation of irradiance at high irradiance levels. However, this effect could be considerable at low irradiance levels.

TABLE I
Extracted Parameters for Different PV Modules at STC

PV Module	$I_{ph,STC}$	$I_{s,STC}$	R_s	R_{sh}	a
ET-M53695	5.581 A	4.14e-10 A	0.2 Ω	97.87 Ω	1.04
BP-4175B	5.46 A	2.89e-08 A	0.329 Ω	164.36 Ω	1.24
JAP6-72-310	8.921 A	1.68e-09 A	0.334 Ω	1668.1 Ω	1.11
KC200GT	8.213 A	9.75e-08 A	0.23 Ω	460.4 Ω	1.31
FS275	1.239 A	1.18e-09 A	8.41 Ω	1117.69 Ω	1.44
NA-E125G5	3.45 A	3.13e-10 A	2.36 Ω	91.6 Ω	1.28

The extracted five parameters of different PV modules at STC are presented in Table I. Dependence of series and shunt resistances on irradiance and temperature is illustrated in Fig. 5. Different PV technologies from different manufacturers were studied. The values are normalized with respect to STC. An increase in irradiance level leads to a decrease in series resistance due to the formation of additional charges, which results in an increase in conductivity of the PV cells [see Fig. 5(b)]. However, the series resistance increases as the temperature increases, as shown in Fig. 5(d), because of a decrease in charge carrier mobility. The parallel resistance behaves rather the same way while experiencing larger magnitude variation. As observed, the resistances depend on both the cell temperature and the insolation level, and their relationship is nonlinear. Furthermore, the variation differs not only among various PV technologies, but also among various manufacturers of the same technology because of different cell configurations.

The series and shunt resistances affect the performance and efficiency of PV modules during operation. Therefore, considering constant values of resistances for a wide range of ambient conditions would cause an error in PV modeling in conventional methods. This is more significant in studies of PV modules under low irradiance or mismatch conditions.

B. Experimental Validation

1) Experimental Setup: To investigate experimentally the effectiveness of the developed model for real operating conditions, tests were carried out on three PV modules with different technologies: an ET-M53695 monocrystalline PV module from ET Solar manufacturer, a CS6P-260P polycrystalline PV module from Canadian Solar manufacturer, and an FS-275 thin-film PV module from First Solar manufacturer. The value of K_{sf} in (8) can be obtained from a comparison between the short-circuit current of the PV panel under test and the short-circuit current data provided by the manufacturer datasheet. The CS6P-260P and FS-275 PV panels are new so that this factor was calculated as almost unity, whereas it was obtained as 0.97 for the ET-M53695.

The experiments were conducted in a field with a latitude of 45.47°, as depicted in Fig 6. The ET-M53695 and CS6P-260P PV modules consist of 36 and 60 series-connected PV cells, respectively, in conjunction with three bypass diodes. On the other hand, the FS-275 PV module comprises 116 PV cells

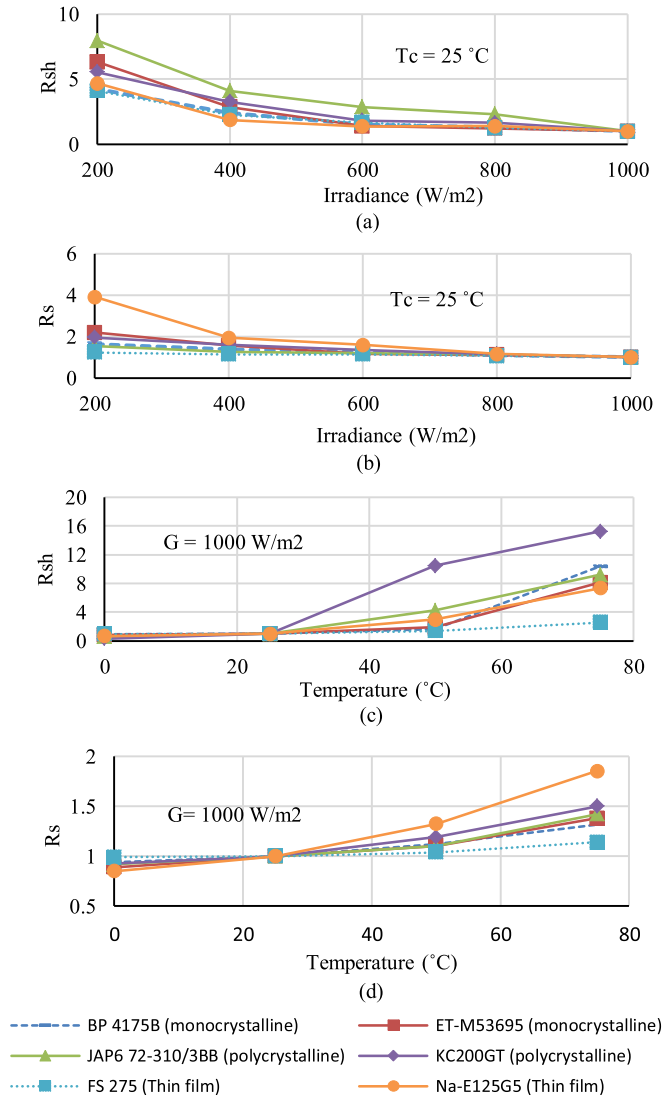

Fig. 5. Effect of irradiance variation on (a) the shunt resistance and (b) the series resistance. Effect of temperature variation on (c) the shunt resistance and (d) the series resistance. The resistance values are normalized with respect to STC.

without bypass diodes. The PV characteristics of the PV panels were measured using HT Instruments *I–V* 400 PV Panel Analyzer and irradiance meter test kit. The PV modules were faced due South during tests with a tilt angle of 30°. The temperature of the back surface of the modules was measured by a Fluke 62 Mini infrared thermometer, which offers quick and reliable surface temperature readings. However, measuring temperature of back surface of the PV modules may not be accurately indicative of the real temperature of the PV cells. The temperature of the p-n junction of the PV module would be then obtained as [25]

$$T_c = T_b + G_{\text{eff}}.\Delta T \tag{21}$$

where T_c is the temperature of the PV module p-n junction, T_b is the temperature of the PV module back surface, and ΔT is the temperature difference between the p-n junction and the PV

Fig. 6. Outdoor experiments of PV modules.

module back surface at the 1000−W/m^2 insolation level. This temperature correction could be considered 3 °C for flat-plate PV modules with an open-rack structure, which was the case in our experiments.

2) Experimental Results: The date and time of the experiments were recorded and entered into the model along with the installation angle to realize the spectral response and reflection losses. By feeding the proposed model with the field information and the manufacturer data, the performance of the PV modules for real outdoor conditions can be predicted.

Estimated *I–V* curves by the proposed modeling technique along with experimental measurements are shown in Fig. 7 for different PV technologies. The circular markers demonstrate the experimental results, while the solid lines in red represent the modeled curves. It is shown that the electrical characteristics and energy production of the PV modules are highly dependent on ambient conditions. There is a good agreement between the experimental measurements and the simulated model in different ambient conditions, with errors of less than 1%. The main source of this error is the instantaneous variation of the irradiance level during the measurements.

C. Comparative Study

The precision of the proposed approach was verified by comparing the modeled *I–V* characteristics of the PV modules with the *I–V* characteristics provided by manufacturer datasheets at different irradiance levels. Verifications were conducted for crystalline and thin-film PV technologies and with reference to the existing models proposed in [7] and [9]. Fig. 8(a) and (b) demonstrates the *I–V* curves of the thin-film Na-E125G5 [9] and the polycrystalline KC200GT [7] PV modules, respectively, at STC and four different irradiance densities. The manufacturer-provided *I–V* curves of the PV modules are shown with circular markers, while the red solid lines represent the *I–V* curves of the proposed approach. The dashed black lines illustrate the *I–V* curves of the previous models, where the parameters were obtained at STC and considered fixed at different conditions.

As can be observed from Fig. 8, there is an obvious mismatch between the manufacturer-provided *I–V* curves and the curves predicted by conventional models when moving away from STC. This mismatch is less considerable in the polycrystalline PV module for which the variation of parameters is smaller,

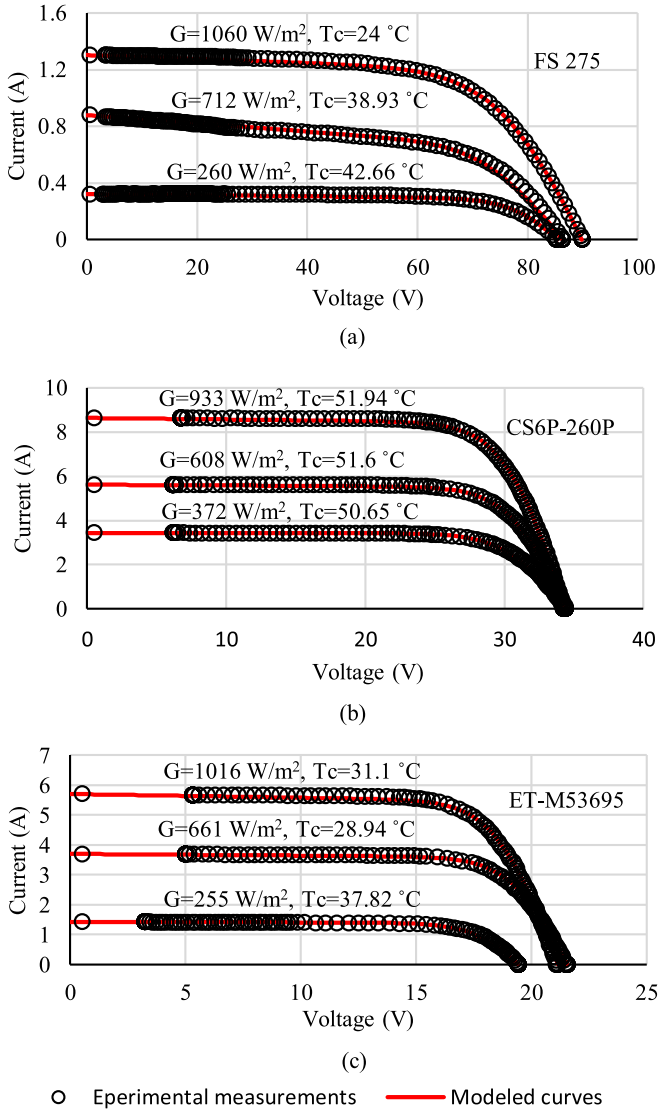

Fig. 7. Modeled and experimentally measured *I–V* curves in different operating conditions for (a) FS-275 (thin film), (b) CS6P-260P (polycrystalline), and (c) ET-M53695 (monocrystalline).

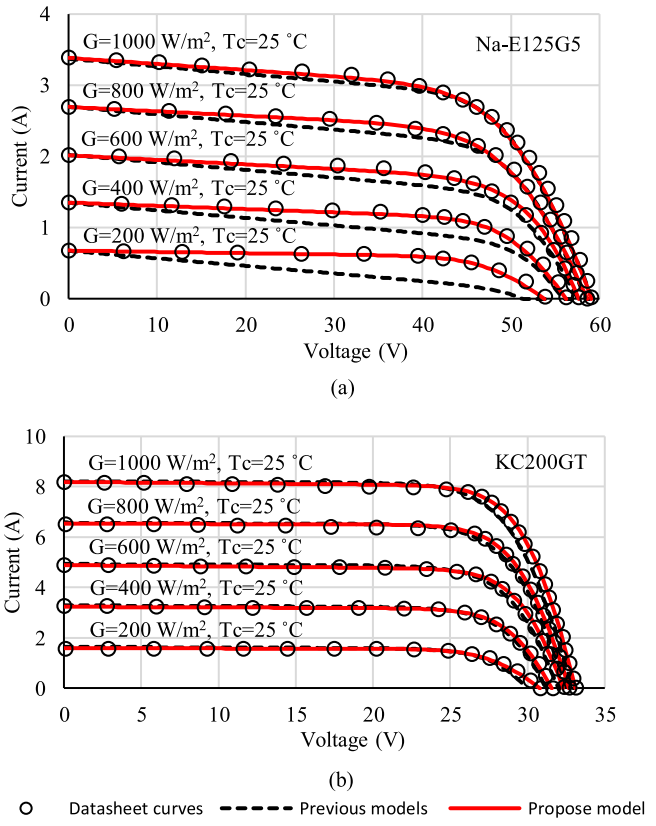

Fig. 8. Comparison with respect to manufacturer-provided *I–V* curves between the proposed model and previous models with constant parameters presented in (a) [9] for the thin-film Na-E125G5 PV module and in (b) [7] for the polycrystalline KC200GT PV module.

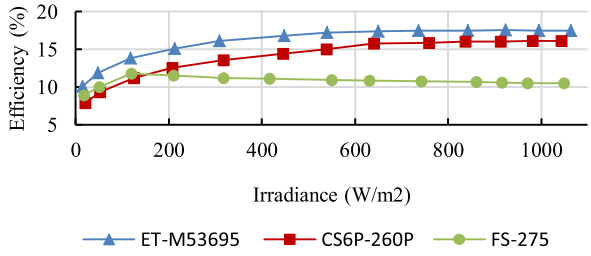

Fig. 9. Efficiency of PV modules as a function of irradiance.

whereas a significant mismatch occurs in the case of thin-film PV module, especially at lower irradiance levels. Nevertheless, larger deviation would be expected at irradiance levels lower than 200 W/m^2, which are common in outdoor conditions. The *I–V* curves of the proposed approach and the manufacturer-provided ones are closely matched at different irradiance levels.

VI. Discussion

It is essential to properly assess the PV modules efficiency and performance because of large investment on PV installations. This could help appropriately evaluate the payback time and would be beneficial for both operation and preconstruction design of PV systems.

Field evaluation of PV modules performance is complicated due to the fact that their efficiency is affected by both temperature and irradiance levels. The effect of temperature on the PV modules efficiency is known and normally reported by manufacturers. The relationship between the MPP and temperature with a constant irradiance could be approximated by a straight line. The slope of this line is interpreted as the temperature coefficient of the output power of the PV module. In practice, this is true for high irradiance levels; however, low irradiance samples are neglected to obtain the temperature coefficient. In fact, the effect of irradiance level on the efficiency of the PV modules is not reported by manufacturer datasheets.

Fig. 9 shows the measured efficiency of the PV modules versus irradiance level. The results are translated to STC temperature of 25 °C. PV cells efficiency is affected by irradiance and deviates from those predicted by manufacturers as the irradiance level decreases. Monocrystalline PV cells generally

TABLE II
ANNUAL ENERGY YIELD OF A 12-MW PV FARM

Year	2013	2014
PV farm SCADA database	14.86 GWh	14.32 GWh
Conventional PV model with uncorrected parameters [7]	15.35 GWh	14.85 GWh
Relative error (%)	3.36%	3.7%
Proposed PV model	14.98 GWh	14.44 GWh
Relative error (%)	0.81%	0.83%

experience higher efficiency as they utilize a broader range of wavelengths of sunlight. The FS-275 thin-film module demonstrates lower variation of efficiency. On the other hand, wider decrease in the efficiency of the CS6P-260P polycrystalline PV module is observed. The extent of PV module efficiency reduction in low irradiance levels depends on the selected PV technology.

The above analysis implies that PV modeling without considering the variation of parameters and efficiency would lead to considerable error in PV energy generation. To realize this error, the energy yield of a 12-MW grid-connected PV farm located in southwest of the city of Ottawa, ON, Canada, was investigated. The results of the simulated models along with the data collected by the SCADA system of the PV farm are shown in Table II. The proposed PV model provides a more precise energy prediction of the PV farm in comparison with the conventional PV model in [7].

As a result, a proper field evaluation requires a more sophisticated understanding of the PV module characteristics than described by manufacturer datasheet. The methodology proposed in this study offers a simple electrical model instead of laborious field measurements to precisely realize the characteristics of PV modules. Moreover, the performance of different PV technologies and configurations for a specific site could be successfully assessed through this model. This enables the proper selection of PV technology and configuration, which leads to an optimum design of the PV installation.

VII. CONCLUSION

This paper has verified the necessity of an accurate PV model, which can predict the real behavior of a PV module under real field conditions. In order to make precise estimations of performance of outdoor-operated PV modules, a more extended investigation of PV characteristics rather than STC parameters is needed. A single-diode PV model along with a parameter extraction procedure has been proposed, which is able to update its parameters. A simple and fast iterative approach has been employed to obtain the series and parallel resistances. A correction on the insolation measurements has been introduced to represent the spectral and optical effects. A good agreement has been achieved between the PV characteristics predicted by the proposed model and those obtained from the manufacturers and experimental measurements.

REFERENCES

[1] S. Mueller, *Next Generation Wind and Solar Power*, Int. Energy Agency, Paris, France, 2016. [Online]. Available: https://www.iea.org/publications/freepublications/publication/NextGenerationWindandSolarPower.pdf

[2] S. Shongwe and M. Hanif, "Comparative analysis of different single-diode PV modeling methods," *IEEE J. Photovolt.*, vol. 5, no. 3, pp. 938–946, May 2015.

[3] E. I. Batzelis, G. E. Kampitsis, S. A. Papathanassiou, and S. N. Manias, "Direct MPP calculation in terms of the single-diode PV model parameters," *IEEE Trans. Energy Convers.*, vol. 30, no. 1, pp. 226–236, Mar. 2015.

[4] V. J. Chin, Z. Salam, and K. Ishaque, "An accurate and fast computational algorithm for the two-diode model of PV module based on a hybrid method," *IEEE Trans. Ind. Electron.*, vol. 64, no. 8, pp. 6212–6222, Aug. 2017.

[5] K. Nishioka, N. Sakitani, Y. Uraoka, and T. Fuyuki, "Analysis of multicrystalline silicon solar cells by modified 3-diode equivalent circuit model taking leakage current through periphery into consideration," *Sol. Energy Mater. Sol. Cells*, vol. 91, no. 13, pp. 1222–1227, 2007.

[6] H. M. Hasanien, "Shuffled frog leaping algorithm for photovoltaic model identification," *IEEE Trans. Sustain. Energy*, vol. 6, no. 2, pp. 509–515, Apr. 2015.

[7] M. G. Villalva, J. R. Gazoli, and E. R. Filho, "Comprehensive approach to modeling and simulation of photovoltaic arrays," *IEEE Trans. Power Electron.*, vol. 24, no. 5, pp. 1189–1208, May 2009.

[8] S. A. Rahman, R. K. Varma, and T. Vanderheide, "Generalized model of a photovoltaic panel," *IET Renew. Power Gener.*, vol. 8, no. 3, pp. 217–229, 2014.

[9] Y. Mahmoud and E. F. El-Saadany, "A photovoltaic model with reduced computational time," *IEEE Trans. Ind. Electron.*, vol. 62, no. 6, pp. 3534–3544, Jun. 2015.

[10] Q. Zhang, H. Liu, and C. Dai, "Fireworks explosion optimization algorithm for parameter identification of PV model," in *Proc. IEEE 8th Int. Power Electron. Motion Control Conf.*, Hefei, China, May 22–26, 2016, pp. 1587–1591.

[11] J. Accarino, G. Petrone, C. A. Ramos-Paja, and G. Spagnuolo, "Symbolic algebra for the calculation of the series and parallel resistances in PV module model," in *Proc. Int. Conf. Clean Elect. Power*, 2013, pp. 62–66.

[12] E. I. Batzelis, I. A. Routsolias, and S. A. Papathanassiou, "An explicit PV string model based on the Lambert W function and simplified MPP expressions for operation under partial shading," *IEEE Trans. Sustain. Energy*, vol. 5, no. 1, pp. 301–312, Jan. 2014.

[13] E. I. Batzelis and S. A. Papathanassiou, "A method for the analytical extraction of the single-diode PV model parameters," *IEEE Trans. Sustain. Energy*, vol. 7, no. 2, pp. 504–512, Apr. 2016.

[14] V. L. Brano, A. Orioli, and G. Ciulla, "On the experimental validation of an improved five-parameter model for silicon photovoltaic modules," *Sol. Energy Mater. Sol. Cells*, vol. 105, no. 2012, pp. 27–39, 2012.

[15] S. Lineykin, M. Averbukh, and A. Kuperman, "Issues in modeling amorphous silicon photovoltaic modules by single-diode equivalent circuit," *IEEE Trans. Ind. Electron.*, vol. 61, no. 12, pp. 6785–6793, Dec. 2014.

[16] M. Hejri and H. Mokhtari, "On the comprehensive parametrization of the photovoltaic (PV) cells and modules," *IEEE J. Photovolt.*, vol. 7, no. 1, pp. 250–258, Jan. 2017.

[17] M. C. D. Piazza, M. Luna, G. Petrone, and G. Spagnuolo, "Translation of the single-diode PV model parameters identified by using explicit formulas," *IEEE J. Photovolt.*, vol. 7, no. 4, pp. 1009–1016, Jul. 2017.

[18] S. Hosseini, S. Taheri, M. Farzaneh, and H. Taheri, "An approach to precise modeling of photovoltaic modules under changing environmental conditions," in *Proc. IEEE Elect. Power Energy Conf.*, Ottawa, ON, Canada, Oct. 12–14, 2016, pp. 1–6.

[19] A. Labouret and M. Villoz, *Solar Photovoltaic Energy*. London, U.K.: Inst. Eng. Technol., 2010.

[20] N. Tanaka, *Technology Roadmap—Solar Photovoltaic Energy*, Photovoltaic Power Syst. Programme, Int. Energy Agency, Paris, France, 2010. [Online]. Available: https://www.iea.org/publications/freepublications/publication/pv_roadmap.pdf

[21] M. Donovan, B. Bourne, and J. Roche, "Efficiency vs. irradiance characterization of PV modules requires angle-of-incidence and spectral corrections," in *Proc. 35th IEEE Photovolt. Spec. Conf.*, Honolulu, HI, USA, Jun. 20–25, 2010, pp. 2301–2305.

[22] J. A. Duffie and W. A. Beckman, *Solar Engineering of Thermal Processes*. New York, NY, USA: Wiley, 2013.

[23] I. Reda and A. Andreas, "Solar position algorithm for solar radiation applications," Nat. Renew. Energy Lab., Golden, CO, USA, Tech. Rep. TP-560-34302, 2008.
[24] G. M. Masters, *Renewable and Efficient Electric Power Systems*. Hoboken, NJ, USA: Wiley, 2013.
[25] D. L. King, W. E. Boyson, and J. A. Kratochvil, Photovoltaic array performance model, Sandia Nat. Lab., Albuquerque, NM, USA, 2004. [Online]. Available: http://prod.sandia.gov/techlib/access-control.cgi/2004/043535.pdf
[26] [Online]. Available: http://www.sandia.gov/pv
[27] C. W. Hansen, Parameter estimation for single diode models of photovoltaic modules, Sandia Nat. Lab., Albuquerque, NM, USA, 2015. [Online]. Available: http://prod.sandia.gov/techlib/access-control.cgi/2015/152065.pdf

Seyedkazem Hosseini (S'15) received the B.Sc. degree in electrical engineering (control) from Tabriz University, Tabriz, Iran, in 2008, and the M.Sc. degree in electrical engineering (power) from the Babol University of Technology, Babol, Iran, in 2012. He is currently working toward the Ph.D. degree with the Université du Québec, Gatineau, QC, Canada.

From 2012 to 2015, he was involved in several projects in power electronics and motor drive systems as a Power Electronics Engineer. His current research interests include renewable energy power conversion especially photovoltaic systems, maximum power point tracking techniques, control of power electronic converters, and adjustable speed drives.

Mr. Hosseini was a recipient of the Research Excellence Scholarship from Hydro-Québec in April 2017.

Shamsodin Taheri (S'11–M'15) received the B.Sc. degree in electrical engineering from the University of Mazandaran, Babolsar, Iran, in 2006, the M.Sc. degree in electrical engineering from the Iran University of Science and Technology, Tehran, Iran, in 2009, and the Ph.D. degree in electrical engineering from the Université du Québec à Chicoutimi, Chicoutimi, QC, Canada, in 2013.

From 2013 to 2014, he was with the Technical Services and Research Department, SaskPower, Regina, SK, Canada. Since 2014, he has been an Assistant Professor with the Université du Québec en Outaouais, Gatineau, QC, Canada. His main research interests include power systems, renewable energy, high voltage, numerical modeling, and transformers.

Masoud Farzaneh (M'83–SM'91–F'07–LF'17) received the Ph.D. degree in electrical engineering from Institut National Polytechnique and Université Paul Sabatier, Toulouse, France, in 1980. Later, in 1986, he obtained a Doctorat d'état ès sciences from Université Paul Sabatier. He has done pioneering research in the field of power engineering, including the impact of cold climate on overhead power networks. He has authored or coauthored more than 700 technical papers and 17 books or book chapters in power engineering. As a mentor, he has trained about 130 postgraduate students and postdoctoral fellows to date.

Prof. Farzaneh was the President of the IEEE Dielectrics and Electrical Insulation Society in 2013, a member of the Editorial Board of the IEEE TRANSACTIONS ON DIELECTRICS AND ELECTRICAL INSULATION, as well as Convenor of CIGRE WG B2 29 and B2.44 on deicing techniques and coatings for protection of overhead lines during winter conditions, and a member of the Executive Committee of CIGRE Canada. He is an Editor-in-Chief of the *IET High Voltage* journal and Convenor of CIGRE WG B2 69 on coatings for power networks. He is a Fellow of the Institution of Engineering and Technology, the Engineering Institute of Canada, and the Canadian Academy of Engineering. His contributions and achievements in research and teaching have been recognized by many prestigious prizes and awards at national and international levels.

Hamed Taheri received the B.Sc. degree in electrical engineering from the University of Mazandaran, Babolsar, Iran, in 2009, and the Ph.D. degree in electrical engineering from the École de Technologie Supérieure, Montréal, QC, Canada, in 2017.

From 2009 to 2011, he was a Research Assistant at the Inverter Quality Control Center, which is responsible for testing photovoltaic inverters that are to be connected to the local utility grid, at the Universiti Teknologi Malaysia, Johor Bahru, Malaysia. Since 2014, he has been a Power Electronic Design Engineer with Primax Technologies Inc., Montréal. His current research interests include power electronics, advanced control, and embedded programming.

Mehdi Narimani (S'09–M'13–SM'15) received the Ph.D. degree in electrical engineering from the University of Western Ontario, London, ON, Canada, in 2012.

He is currently an Assistant Professor with the Department of Electrical and Computer Engineering, McMaster University, Hamilton, ON. Prior joining McMaster University, he was a Power Electronics Engineer with Rockwell Automation Canada, Cambridge, ON. He has authored/coauthored more than 60 journal and conference proceeding papers, coauthored a Wiley-IEEE Press book, and holds more than four issued/pending U.S./European patents. His current research interests include power conversion, high-power converters, control of power electronics converters, and renewable energy systems.